Management of autofluorescence in formaldehyde-fixed myocardium: choosing the right treatment

Zhao Zhang, 1 Hongming Fan, 1 William Richardson, 2 Bruce Z. Gao, 1 Tong Ye1,3

Autofluorescence (AF) poses challenges for detecting proteins of interest in situ when employing immunofluorescence (IF) microscopy. This interference is particularly pronounced in strongly autofluorescent tissues such as myocardium, where tissue AF can be comparable to IF. Although various histochemical methods have been developed to achieve effective AF suppression in different types of tissue, their applications on myocardial samples have not been well validated. Due to inconsistency across different autofluorescent structures in some types of tissue, it is unclear if these methods can effectively suppress AF across all autofluorescent structures within the myocardium. Here, we quantitatively evaluated the performance of several commonly used quenching treatments on formaldehyde-fixed myocardial samples, including 0.3 M glycine, 0.3% Sudan Black B (SBB), 0.1% and 1% sodium borohydride (NaBH₁), TrueVIEW® and TrueBlack®. We further assessed their quenching performance by employing the pre-treatment and post-treatment protocols, designed to cover two common IF staining scenarios where buffers contained detergents or not. The results suggest that SBB and TrueBlack® outperform other reagents in AF suppression on formaldehyde-fixed myocardial samples in both protocols. Furthermore, we inspected the quenching performance of SBB and TrueBlack® on major autofluorescent myocardial structures and evaluated their influence on IF imaging. The results suggest that SBB outperforms TrueBlack® in quenching major autofluorescent structures, while TrueBlack® excels in preserving IF labeling signal. Surprisingly, we found the treatment of NaBH₄ increased AF signal and enhanced the AF contrast of major autofluorescent structures. This finding suggests that NaBH4 has the potential to act as an AF enhancer and may facilitate the interpretation of myocardial structures without the need for counterstaining.

Key words: immunofluorescence; autofluorescence suppression; autofluorescence enhancement; myocardium; formaldehyde.

Correspondence: Tong Ye, Department of Bioengineering, Clemson University, 68 President Street, MSC 501, Charleston, SC 29425, South Carolina, USA. E-mail: ye7@clemson.edu

Contributions: all the authors made a substantive intellectual contribution, read and approved the final version of the manuscript and agreed to be accountable for all aspects of the work.

Conflict of interest: the authors declared no potential conflicts of interest concerning the research, authorship, and publication of this article.

Ethical approval: the animal protocol listed below has been reviewed and approved by the Institutional Animal Care and Use Committee (IACUC) of the Medical University of South Carolina (no. IACUC-2019-00868).

Availability of data and materials: the datasets used and analyzed in this study are available from the corresponding author on reasonable request.

Funding: this research was supported by South Carolina IDeA Networks of Biomedical Research Excellence (SC INBRE), a National Institutes of Health (NIH) funded center (Award P20GM103499), MTF Biologics Extramural Research Grant, South Carolina Translation Research Improving Musculoskeletal Health (TRIMH), an NIH funded Center of Biomedical Research Excellence (Award P20GM121342), and an R01 research grant to BG and WR (R01HL144927). This work was partly supported by the National Science Foundation EPSCoR Program under NSF Awards OIA-1655740 and OIA-2242812.



¹Department of Bioengineering, Clemson University, Clemson, SC

²Department of Chemical Engineering, University of Arkansas, Fayetteville, AR

³Department of Regenerative Medicine and Cell Biology, Medical University of South Carolina, Charleston, SC, USA



Introduction

Immunofluorescence (IF) microscopy is an indispensable tool to visualize proteins of interest and detect protein interactions *in situ* using fluorophores conjugated antibodies. The characterization and evaluation of proteins through qualitative observation and quantitative analysis of IF images play a critical role in studying the molecular basis of disease pathogenesis, signaling pathways, and therapeutic responses.¹⁻⁵ Unfortunately, IF labeling is often interfered with autofluorescence (AF) when performing multicolor staining or using fluorescent dyes with excitation/emission spectra similar to tissue AF. Crosstalk and comparable signal levels between IF labeling and tissue AF disturb the detection and localization of target proteins. Accordingly, suppression of AF is necessary to maintain the efficiency and accuracy of protein detection in IF microscopy.

Tissue AF arises from a mixture of endogenous fluorophores, and its characteristics depend on the distribution and concentration of these fluorophores. Ubiquitous endogenous fluorophores include nicotinamide adenine dinucleotide (NADH and its phosphate analog NADPH), flavoproteins, lipofuscin, elastin, and collagen. Although each type of endogenous fluorophore has its distinctive emission spectrum, when tissue samples are excited with short wavelengths (UV or blue), the collective emission spans the entire visible spectral range.6 In addition, fixatives are considered as a major factor affecting AF in tissue samples. Formaldehyde is the most commonly used fixative due to its ease of handling and availability. Formaldehyde preserves cellular and extracellular components of tissues by reacting with proteins and forming cross-links. During the formaldehyde fixation process, amine condensation reactions can yield strongly fluorescent products.7 Upon excitation with UV or blue light, the emission of formaldehyde itself8 along with its cross-links7 covers the entire visible range. Generally, selecting longer excitation wavelengths can reduce AF originating from both sources. However, this approach restricts the selection of fluorescent dyes, making it impractical for the detection of multiple antigens.

Some histochemical approaches have been developed to suppress AF in formaldehyde-fixed tissue samples. Sodium borohydride (NaBH₄) has been reported to reduce AF in neural⁹ and respiratory¹⁰ tissues by reducing Schiff bases formed during formaldehyde cross-linking. Schiff bases formed during formaldehyde cross-linking. Sudan Black B (SBB) has been suggested to suppress AF in various types of tissue, including bone marrow/cartilage, neural, sale renal, style pancreatic, and intestinal tissues. Glycine has been typically used to quench reactions of free or protein-conjugated formaldehyde in chromatin immunoprecipitation and protein-protein interaction studies. Several commercial products have recently been developed to

mask autofluorescent structures utilizing a quenching mechanism similar to SBB. For instance, TrueBlack® lipofuscin autofluorescence quencher (Biotium, Fremont, CA, USA) was used to quench AF in formaldehyde-fixed cardiac tissues.²¹⁻²³ However, the lack of comparative studies in the context of myocardial samples limits our knowledge of the efficacy and suitability of different quenching treatments. Moreover, previous studies have indicated that these histochemical treatments have varying quenching performance across different autofluorescent structures within tissues.^{10,12,14,18} As such, it remains unclear whether these treatments would be equally effective for all autofluorescent structures within the myocardium.

This study aims to comparatively study the quenching performance of different histochemical treatments on formaldehydefixed myocardial samples and investigate their effectiveness across different autofluorescent structures within the myocardium. We intend to provide practical suggestions on selecting proper histochemical approaches to manage AF in myocardial samples during IF staining experiments. First, we quantitatively evaluated the performance of commonly available quenching treatments on formaldehyde-fixed myocardial samples and assessed the influence of application protocols on their quenching performance. Second, we identified major autofluorescent structures in formaldehyde-fixed myocardial samples by IF staining, with an emphasis on the typical histological structures within the myocardium, including mitochondria (via mitochondrial outer membrane protein, VDAC1), microvascular endothelial cells (via endothelial marker, CD31), basement membrane (via collagen type IV, ColIV), and cardiac interstitium (via collagen type I, ColI, and collagen type III, ColIII). Finally, we examined the quenching performance of these treatments on identified autofluorescent structures and inspected their impact on IF imaging.

Materials and Methods

Chemicals and antibodies

All the following chemicals were purchased from MilliporeSigma (Burlington, MA, USA): sodium borohydride (NaBH₄), Sudan Black B (SBB), glycine, paraformaldehyde (PFA), sucrose, isopentane, phosphate buffered saline (PBS), Triton X-100, and bovine serum albumin (BSA). Additional chemicals used in this study include TrueBlack® (Biotium), TrueVIEW® (Vector Laboratories, Newark, CA, USA), and Mowiol 4-88 (Polysciences; Warrington, PA). Detailed information on primary and secondary antibodies is listed in Table 1.

Table 1. List of antibodies used in the study.

Antigen (origin)	Dilution	Product no.	Vendor
VDAC1 (rabbit)	1:200	ab15895	Abcam
CD31 (rat)	1:100	DIA-310	Dianova
Collagen type I (rabbit)	1:200	600-401-103	Rockland
Collagen type III (rabbit)	1:200	600-401-105	Rockland
Collagen type IV (rabbit)	1:200	ab19808	Abcam
Secondary antibody (origin)	Dilution	Product no.	Vendor
Anti-rabbit IgG STAR RED (goat)	1:500	STRED	Abberior
Anti-rat IgG, biotinylated (goat)	1:100	BA-94015	Vector Lab.
Streptavidin, Cy5	1:100	SA-1500-1	Vector Lab.





Tissue sections

All procedures and animal care (protocol number, IACUC-2019-00868) were approved by the Institutional Animal Care and Use Committee (IACUC) of the Medical University of South Carolina. Ventricles were isolated from the hearts of C57BL/6 mice, fixed in freshly prepared 4% (w/v) PFA, cryoprotected by sucrose solution, then snap-frozen in liquid nitrogen cooled isopentane. Frozen blocks were consecutively sliced into 10 µm-thick sections and mounted on microscope slides (VWR International, Radnor, PA, USA).

Immunofluorescence staining

Heat-induced antigen retrieval was performed by incubating sections in sodium citrate pH 6.0 at 95°C for 20 min. Sections were blocked in 2% (w/v) BSA with/without 0.3% Triton X-100 at room temperature, then incubated with primary antibodies at 4°C overnight. Sections were incubated with secondary antibodies at room temperature for 3 h. CD31 was detected by avidin-biotin complex (Cy5-conjugated streptavidin; Vector Laboratories). After staining, sections were mounted in Mowiol medium and coverslipped. Primary and secondary antibodies were diluted in the blocking buffer. Negative primary antibody controls were performed to confirm that the staining signal was from the detection of target antigens.

Autofluorescence quenching

The performance of commonly available quenching treatments was initially evaluated on unstained sections, including 0.3 M glycine, 0.3% SBB, 0.1% and 1% NaBH₄, as well as two commercial products, TrueVIEW® and TrueBlack®. Details of these treatments are summarized in Table 2. To evaluate the impact of application protocols on the quenching performance of these treatments and explore potential pitfalls during IF staining, the pre- and posttreatment protocols were utilized to apply the treatments to immunostained samples (immunostaining of ColIV). In the pretreatment protocol, samples were treated with quenching reagents before the blocking step, and all buffers in the following steps were detergent-free. In the post-treatment protocol, samples were treated with quenching reagents after the staining, where blocking and wash buffers contained detergent (Triton X-100 was used as the detergent in this study). All quenching reagents were freshly prepared within 2 h before treatment. For each sample subjected to a particular quenching treatment, a control sample was prepared using its consecutive section where the quenching reagent was omitted.

Confocal laser scanning system

Confocal imaging experiments were performed on a home-built multimodal microscope.²⁴ Briefly, two picosecond pulsed lasers (470 nm and 635 nm, PicoQuant, Berlin, Germany) were synchronized, serving as excitation. Two excitation lasers (FF662-

FDi01 and Di02-R488; Semrock, Rochester, NY, USA) were combined by dichroic mirrors, deflected by a scanning unit consisted of an XY two-axis galvanometer set (8310K; Cambridge Technology, Atlanta, GA, USA), expanded by a lens pair (89683; Edmund Optics, Barrington, NJ, USA; TTL200, Thorlabs, Inc., Newton, NJ, USA), directed to the back aperture of a HCX Plan Apo 63x oil NA 1.40 objective (Leica Microsystems, Wetzlar, Germany). For the detection of green fluorescence (CH1), the emission light was spectrally separated from the excitation lights and red fluorescence by dichroic mirrors (Di02-R488, FF662-FDi01 and FF624-Di01; Semrock), filtered by a bandpass filter (FF01-525/50; Semrock), coupled into a multimode fiber (Thorlabs), and detected by a single photon counting module (SPCM-AQRH-13; Excelitas Technologies Corp., Waltham, MA, USA). For the detection of far-red fluorescence (CH2), the emission light was spectrally separated from the excitation lights and green fluorescence by dichroic mirrors (Di02-R488, FF662-FDi01 and FF735-Di01; Semrock), filtered by a bandpass filter (690/50; Chroma, Bellows Falls, VT, USA), coupled into a multimode fiber (Thorlabs), and detected by a single photon counting module (SPCM-AQRH-13; Excelitas Technologies Corp.).

Image acquisition and processing

For AF imaging, the excitation laser at 470 nm was used. AF images were acquired at CH1 with an emission range of 525±25 nm and CH2 with an emission range of 690±25 nm. For IF imaging of Cy5- or STAR RED-labeled proteins, the excitation laser at 635 nm was used. IF images were acquired at CH2 with an emission range of 690±25 nm.

All samples were imaged under the same experimental conditions of excitation and detection. Image acquisition was executed through SciScan (Scientifica, Brambleside, Uckfield, UK), and image processing was conducted using a custom-developed MAT-LAB algorithm. Raw images were acquired in 16-bit grayscale and frame-averaged to reduce random noise. No image processing was applied to AF images utilized for the quantitative evaluation of the quenching performance of treatments. To facilitate the identification of autofluorescent structures, Wiener smoothing (kernel size, 3x3) and contrast stretching were applied to both IF and AF images before merging them. When studying the quenching performance of treatments on identified autofluorescent structures, histogram matching was conducted independently for both IF and AF images of treated samples. Their histograms were adjusted to match the histograms of the images from the corresponding control.

Image analysis

The image-based metrics were used for quantitative evaluation of quenching performance.

Measurements from the images were obtained using a customdeveloped macro in Fiji (ImageJ, National Institutes of Health). From each treated and untreated (negative-treatment control) sample, ten regions of interest (ROIs) were imaged and analyzed. ROIs

Table 2. List of histochemical quenching treatments evaluated in the study.

Reagents	Time	Notes
0.3 M Glycine	30 min	
0.3% (w/v) SBB	30 min	Sections may dry out during the incubation
0.1% (w/v) NaBH ₄	10 min (3 times)	NaBH ₄ solution should be ice-cooled
1% (w/v) NaBH ₄	10 min (3 times)	NaBH ₄ solution should be ice-cooled
TrueVIEW®	5 min	
TrueBlack®	5 min	Sections may dry out during the incubation





were selected based on the criterion that at least 80% of fields of view contained myocardial structures. In each ROI, a mean grayscale value was measured to represent the AF signal in that ROI. The AF signal in treated and untreated samples was calculated from ten ROIs (n=10) and reported as mean \pm SD. AF signal baselines were established for the performance comparison among different treatments using the same application protocol (pre- or post-treatment). Baselines were calculated as the average AF signal of all the controls that underwent the same application protocol. Statistical differences were calculated using unpaired two-tailed t-tests in Prism (GraphPad Software), and a significance level of p<0.05 was considered statistically significant.

Results

Quantitative performance evaluation of autofluorescence quenching treatments on formaldehydefixed myocardial samples

We first evaluated six histochemical quenching treatments on unstained formaldehyde-fixed myocardial sections, including 0.3 M glycine, 0.3% SBB, 0.1% NaBH₄, 1% NaBH₄, TrueVIEW®, and TrueBlack®. All treatments, except for the glycine one, resulted in significant changes in AF signals detected by CH1 (525±25 nm) and CH2 (690±25 nm) upon excitation of 470 nm (Figure 1). Notably, AF signal in CH1 changed more pronouncedly than in CH2. Treatments with SBB, TrueVIEW®, and TrueBlack® led to a decrease in AF signals, while 0.1% and 1% NaBH₄ increased AF signals in both channels. To assess their performance on immunostained samples, we conducted a further evaluation on ColIV-immunostained myocardial sections. In this evaluation, only treatments that resulted in significant changes in AF signals on unstained samples were included. In addition, we investigated

whether the quenching performance of these treatments could be affected by different application protocols. The pre-treatment and post-treatment protocols were included to cover two common scenarios of IF staining. The post-treatment protocol is designed to accommodate scenarios where IF procedures involve the use of detergent-containing buffers, while the pre-treatment protocol is intended for detergent-free IF staining. As shown in Figure 2, AF signals in both channels are significantly reduced after SBB, TrueVIEW®, and TrueBlack® treatments in both pre-treatment (Figure 2A, all p-values < 0.001) and post-treatment (Figure 2B, all p-values <0.0001) protocols. In contrast, AF signals in both channels are significantly increased after NaBH4 treatments except for 0.1% NaBH₄ treatment in CH2. These results are in line with the findings on unstained sections. To compare the quenching performance among different treatments, we calculated the relative change of AF signals for each treatment, using AF signal baselines as references (see Materials and Methods). The relative changes of AF signals, expressed in an arbitrary unit of grayscale values, are reported in Table 3. Samples treated with SBB and TrueBlack® using the pre-treatment protocol had a greater decrease in AF signals compared to samples treated with TrueVIEW®. Similarly, samples treated with SBB and TrueBlack® using the post-treatment protocol also showed a greater reduction in AF signals. In contrast, samples treated with 0.1% and 1% NaBH₄ using the pre-treatment protocol showed positive relative changes in CH1, while their relative changes in CH2 were comparable. When using the post-treatment protocol, 1% concentration outperformed 0.1% concentration in both channels.

Structure-dependent autofluorescence quenching performance on formaldehyde-fixed myocardial samples

To inspect the quenching performance of treatments on specific autofluorescent structures, we first identified major structures within formaldehyde-fixed myocardial samples that emitted

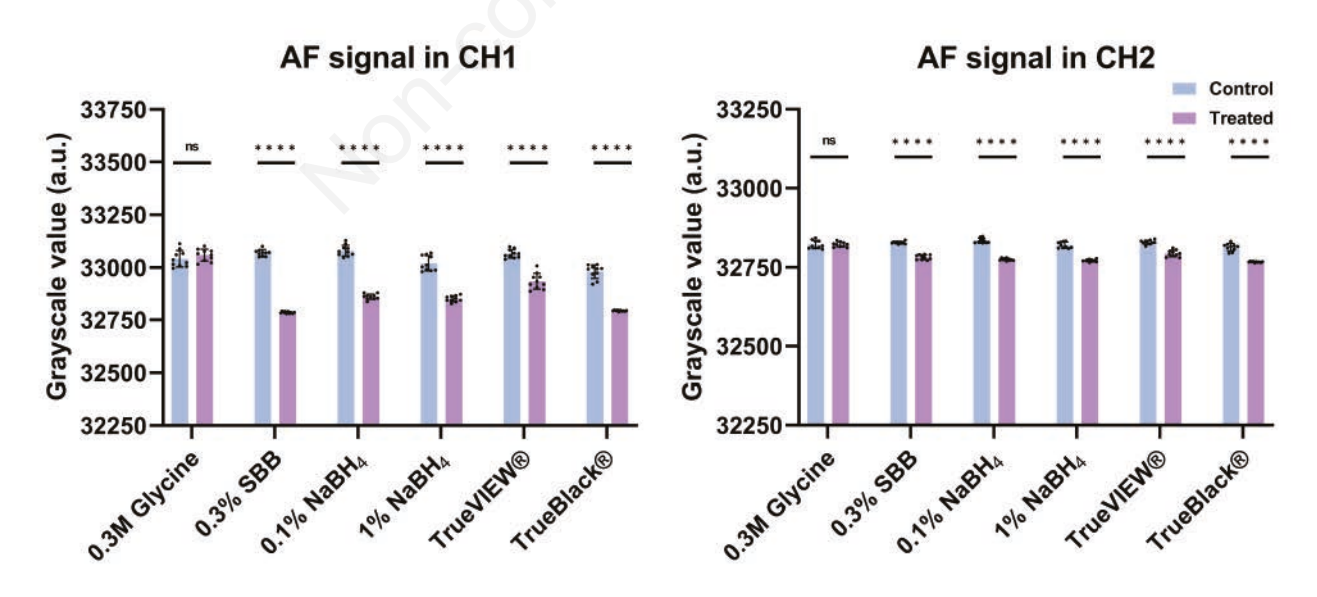


Figure 1. Quantitative evaluation of 0.3 M glycine, 0.3% SBB, 0.1% NaBH₄, 1% NaBH₄, TrueVIEW®, and TrueBlack® treatments on unstained formaldehyde-fixed mouse myocardial samples. AF was excited at 470 nm, detected at CH1 (525±25 nm) and CH2 (690±25 nm). Each treated sample subjected to a specific treatment had its own control (treatment-omitted consecutive section). Statistical analysis was performed between each pair of control and treated samples. Error bars represent standard deviation of each dataset (n=10); two-tailed Student's *t*-tests; ns, not significant, ****p<0.0001.



Table 3. AF signal levels in CH1 and CH2, and relative changes to AF signal baselines. All results are expressed in an arbitrary unit of grayscale values calculated from 16-bit images.

Application protocols	Samples (n=10)	AF Signal in CH1		AF Signal in CH2	
		Mean ± SD	Relative change	Mean ± SD	Relative change
Pre-treatment	Baseline (n=50)	33189		32,905	
	0.3% SBB	32,780±3.6	-409	32,765±4.7	-140
	0.1% NaBH ₄	33,275±35	86	32,941±17	36
	1% NaBH ₄	33,347±44	158	32,945±17	40
	TrueVIEW®	33,132±34	-57	32,898±12	-7
	TrueBlack®	32,830±11	-359	$32,778\pm4.4$	-127
Post-treatment	Baseline (n=50)	33,069		32,884	
	0.3% SBB	$32,789 \pm 4.5$	-280	$32,786 \pm 8.8$	-98
	$0.1\%~\mathrm{NaBH_4}$	33,222±20	153	32,893±9.5	9
	1% NaBH ₄	$33,251 \pm 39$	182	32,928±15	44
	TrueVIEW®	32,943±26	-126	32,820±12	-64
	TrueBlack®	32,811±7.8	-258	32,772±5.0	-162

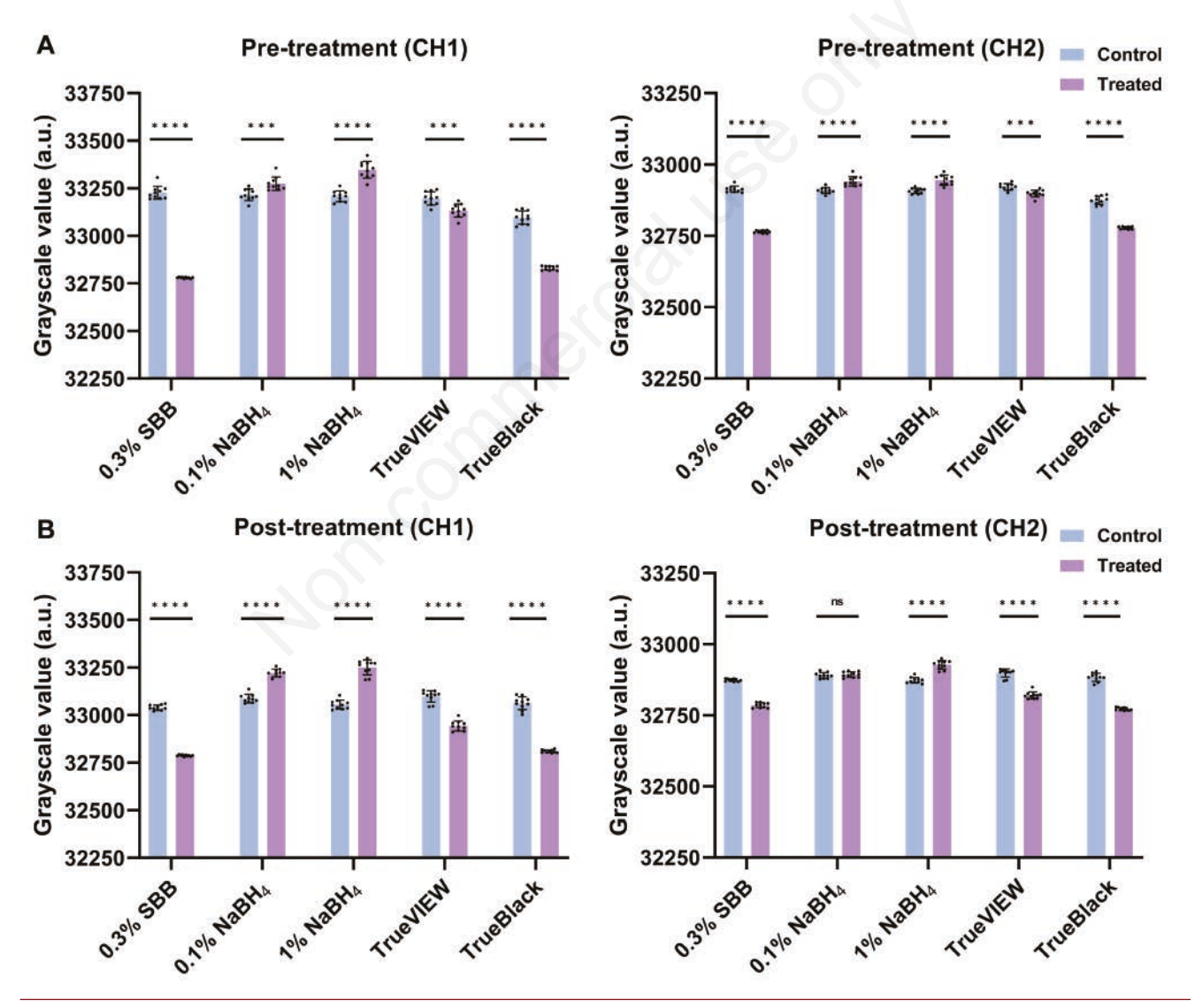


Figure 2. Quantitative evaluation of 0.3% SBB, 0.1% NaBH₄, 1% NaBH₄, TrueVIEW®, and TrueBlack® treatments on immunostained formaldehyde-fixed mouse myocardial samples using (**A**) pre-treatment and (**B**) post-treatment application protocols. Each treated sample subjected to a specific treatment had its own control (treatment-omitted consecutive section). Statistical analysis was performed between each pair of control and treated samples. Error bars represent standard deviation of each dataset (n=10); two-tailed Student's *t*-tests; ns, not significant, ***p<0.001, ****p<0.0001.



imageable AF. IF stainings were performed to localize basement membrane, mitochondria, endothelial cells, and cardiac interstitium by targeting ColIV, VDAC1, CD31, ColI, and ColIII. It should be noted that we previously observed that sarcomeres did not generate visible AF contrast using a two-photon imaging system.24 Therefore, the staining of sarcomeric structures was not considered in this work. Representative IF and AF images were postprocessed with Wiener smoothing and contrast stretching for visualization purposes (Figure 3). Major autofluorescent myocardial structures were identified by merging IF (displayed in red) and AF (displayed in green) images of the same ROIs. ColIV, the fundamental building block of basement membrane, surrounds cardiomyocytes and microvascular endothelial cells. Within the ColIV-delineated areas, there are two distinct patterns in AF images (Figure 3A). To further distinguish between cardiomyocytes and microvessels, mitochondria and endothelial cells were stained. The bright clusters surrounded by basement membrane were identified as mitochondria in cardiomyocytes (Figure 3B). The appearance of mitochondria in cardiomyocytes observed in AF images is consistent with the fact that they are densely packed between myofibrils, occupying a substantial fraction of cardiomyocyte volume (at least 30%).25 ColIV-surrounded regions with a smaller area that typically appear as black holes were identified as microvessel lumens (Figure 3C). Notably, the oval-to-rectangular regions in cardiomyocytes lacking visible AF contrast could be cardiomyocyte nuclei26 (marked by star signs in AF images of Figure 3 A,B). In addition, the bright objects within vessel lumens in AF images could be attributed to erythrocytes (marked by arrowheads in IF images of Figure 3 A,C). Figure 3 D,E shows cardiac endomysium and perimysium detected by IF stainings of ColI and ColIII, predominant components of the cardiac interstitial matrix.²⁷ In AF images, the endomysial and perimysial layers are not visible, showing narrow black gaps surrounding individual cardiomyocytes and cardiomyocyte bundles. It is observed that ColI densely surrounds capillaries (Figure 3D). Due to the limited spatial resolution, the interstitial collagen network, which is known to enclose individual capillaries, cannot be visually distinguished from capillary walls. In contrast, ColIII shows more prominent contrast in the inner layer beneath the endocardial surface, while this layer is not visible in the AF image (Figure 3E).

We then inspected the effectiveness of SBB and TrueBlack®, which were previously shown to be the most efficient quenching

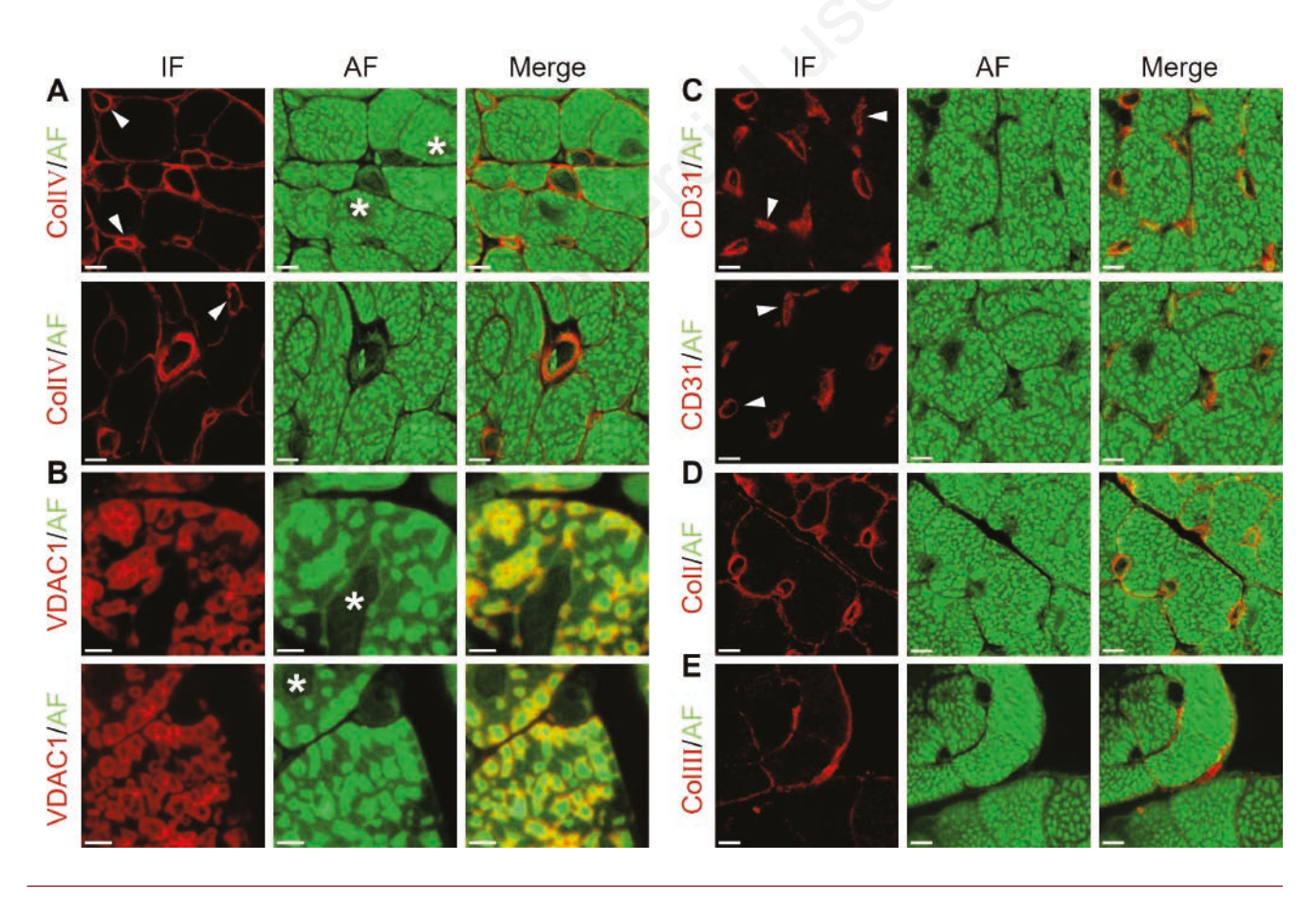


Figure 3. Major autofluorescent structures in formaldehyde-fixed mouse myocardial samples identified by IF stainings of (A) ColIV, (B) VDAC1, (C) CD31, (D) ColI, and (E) ColIII. Images were acquired at cardiomyocyte cross-sectional areas. IF staining (red) allows the localization of basement membrane (ColIV), mitochondria (VDAC1), microvascular endothelial cells (CD31), and interstitial collagen network (ColI and ColIII), facilitating the identification of observable structures in AF images (green) acquired at CH1 (525±25 nm). Oval-to-rectangular nuclei (star signs) are observed within cardiomyocytes, and erythrocytes are present within some capillaries (arrowheads). Scale bars: A,C-E) 5 μm; B) 2 μm.



treatments in this study, on IF-identified autofluorescent structures within the myocardium. In addition, we examined their impact on IF staining signal. 1% NaBH₄ treatment was also included due to its unique AF enhancement effect (outperformed 0.1% concentration as indicated by the previous results). Figures 4 and 5 show confocal IF and AF images of formaldehyde-fixed myocardial samples (ColIV-immunostained) treated with SBB, TrueBlack®, and NaBH₄ using the pre-treatment and post-treatment protocols, respectively. For an overall examination of the AF quenching performance, large-FOV IF and AF images were acquired using wide-

field fluorescence microscopy (Supplementary Figures S1 and S2).

In the pre-treatment protocol (Figure 4), IF staining signal was preserved with TrueBlack® but significantly reduced with SBB. Under SBB treatment, major autofluorescent structures are invisible in both CH1 and CH2, leaving only a dim and uneven tissue background with no discernible features (Figure 4B). In the sample treated with TrueBlack®, AF features in cardiomyocytes are less prominent than those in microvessels but remain recognizable (Figure 4C). In contrast, NaBH₄ treatment not only effectively preserved IF staining signal but also enhanced AF contrast in both

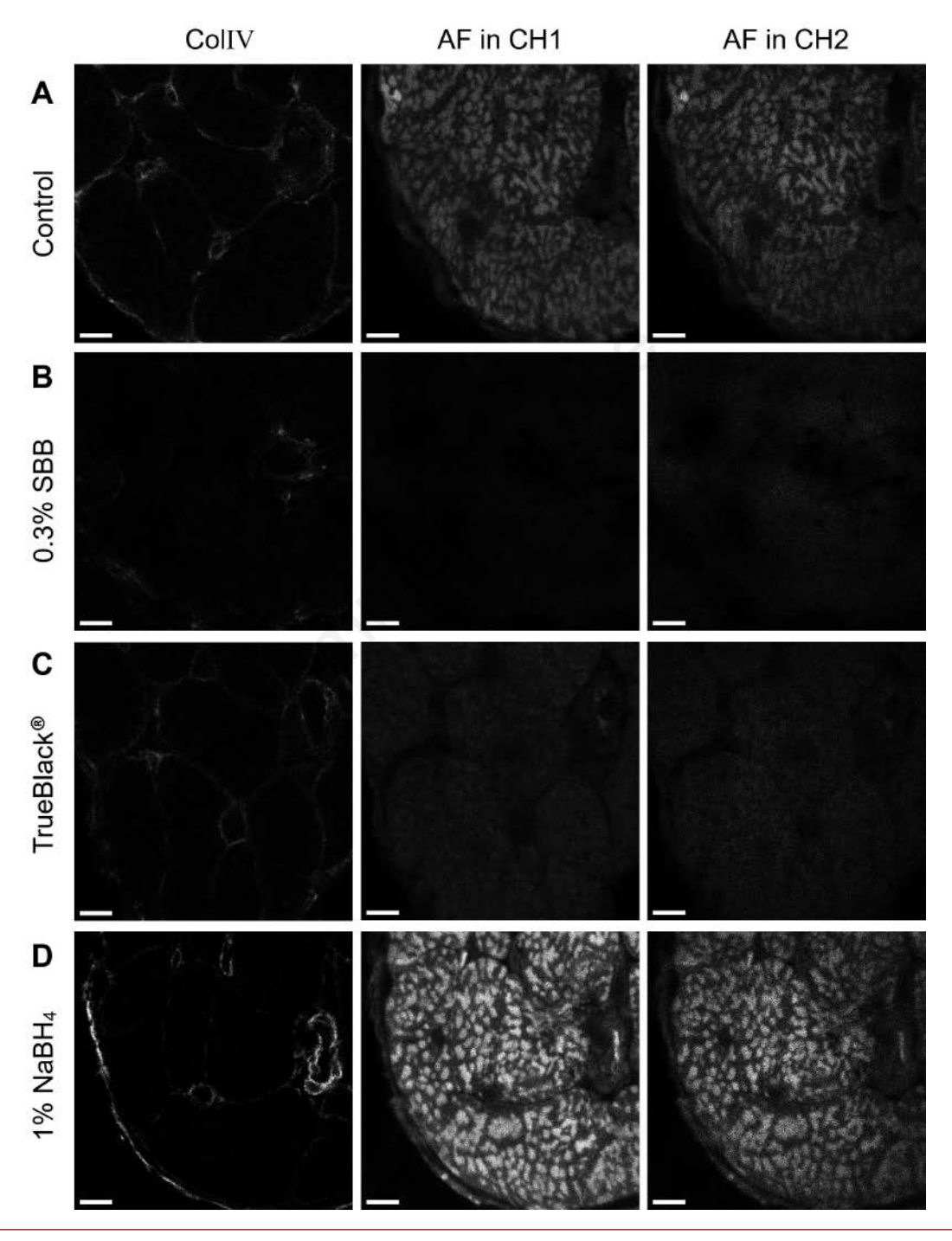


Figure 4. Confocal IF and AF images of (A) control and samples treated with (B) 0.3% SBB, (C) TrueBlack[®], and (D) 1% NaBH₄ using the pre-treatment application protocol. Scale bars: 5 μm. Histogram matching was conducted independently for both IF and AF images of treated samples, using the corresponding IF and AF control images as references.





CH1 and CH2, making autofluorescent structures such as mitochondria, microvessels, and endocardial layer much clearer (Figure 4D).

In the post-treatment scenario (Figure 5), TrueBlack® effectively preserved IF staining signal, whereas SBB failed to do it. Both SBB and TrueBlack® treatments rendered all major autofluorescent structures indiscernible, leaving only a tissue background (Figure 5 B,C). Nevertheless, TrueBlack® resulted in a uniform tis-

sue background, while SBB generated a background with irregular black regions. In contrast, $NaBH_4$ treatment improved the clarity of major autofluorescent structures, especially in CH1. However, the application of $NaBH_4$ using the post-treatment protocol failed to preserve IF staining signal, which was diminished to a low-visible level (Figure 5D).

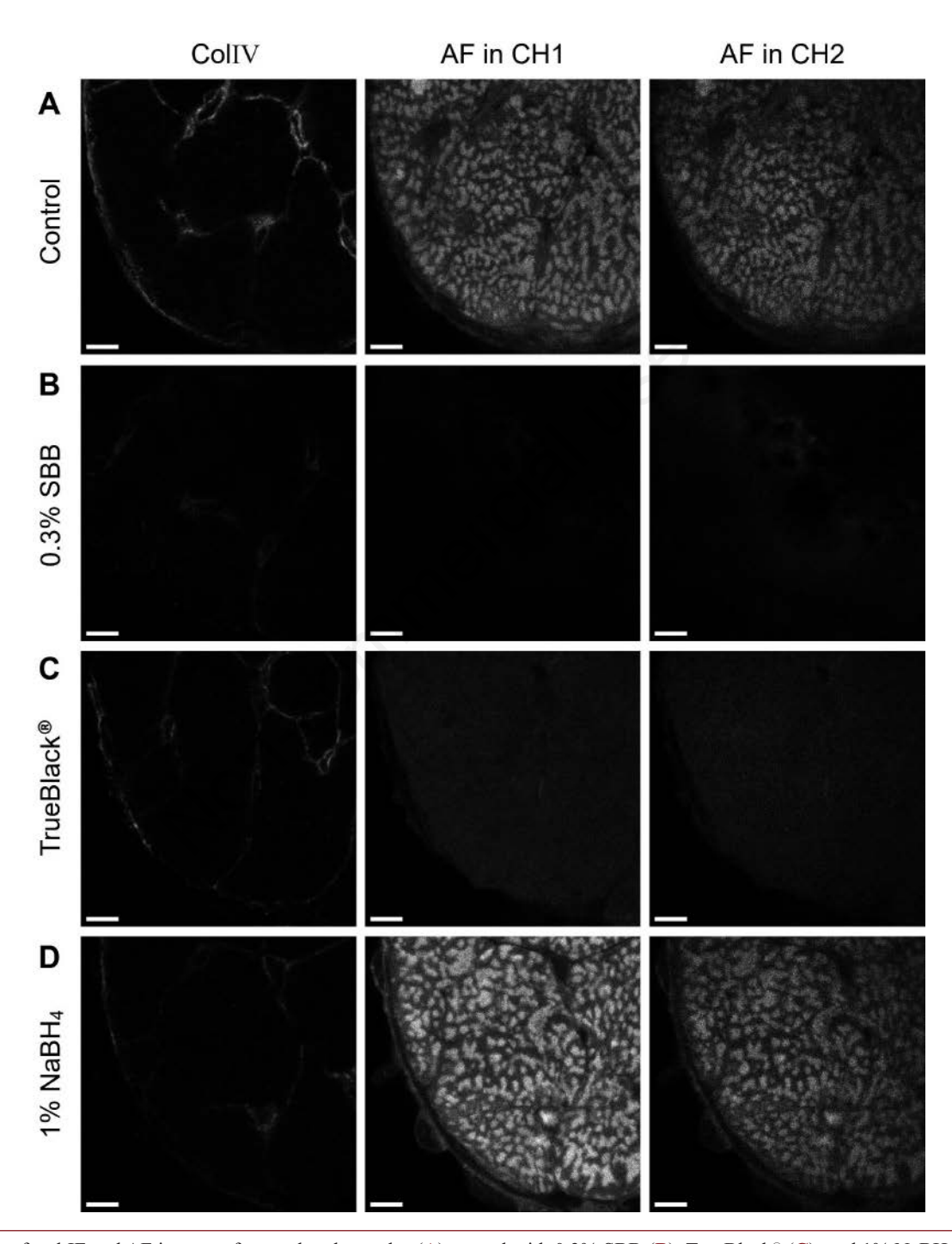


Figure 5. Confocal IF and AF images of control and samples (A) treated with 0.3% SBB (B), TrueBlack® (C), and 1% NaBH₄ (D) using the post-treatment application protocol. Scale bars: 5 μ m. Histogram matching was conducted independently for both IF and AF images of treated samples, using the corresponding IF and AF control images as references.



Discussion

We have evaluated several commonly used histochemical quenching treatments, including 0.3 M glycine, 0.3% SBB, 0.1% and 1% NaBH₄, TrueVIEW®, and TrueBlack®, for suppressing AF in formaldehyde-fixed myocardial samples. The treatments of 0.3% SBB for 30 min and TrueBlack® for 5 min demonstrated the highest efficiency in suppressing AF in formaldehyde-fixed myocardium, according to the quantitative evaluations conducted on unstained and immunostained myocardial samples. TrueBlack® is a convenient, ready-to-use solution, while the preparation of a clear SBB solution takes some time. TrueBlack® requires a shorter incubation period with a slightly lower quenching efficiency than SBB. Although a longer incubation may improve the quenching performance of TrueBlack® further, an incubation time of 5 min has proved to be sufficient. It is important to note that samples should be regularly checked to prevent sections from drying out during SBB and TrueBlack® treatments. Although TrueVIEW® has been used to suppress AF in various formaldehyde-fixed tissues such as spleen, pancreas, aorta, liver, skin, and lung,28,29 its efficiency was found to be lower than SBB and TrueBlack®, making it a suboptimal choice for AF quenching in myocardial samples.

Removing excess quenching reagents after treatments is crucial to avoid reagent-induced background. Although wash buffers containing detergent are beneficial for removing free reagents, they can also wash out functional reagents and reduce quenching efficiency. All reagents showed no significant changes in AF signals in both channels when treatments were applied before the blocking step, and buffers containing detergent were used in the subsequent steps (not shown). When performing IF staining that requires permeabilization, it is recommended to perform SBB, TrueBlack®, and TrueVIEW® treatments after the permeabilization step, and the use of detergents should be avoided in the following steps.

Glycine has been used to quench formaldehyde reactions in chromatin immunoprecipitation³⁰ and immunoaffinity chromatography³¹. It is generally accepted that glycine can react with both free formaldehyde and formaldehyde-modified residues on proteins, effectively blocking formaldehyde cross-linking reactions; 19,20 hence, formaldehyde-induced AF can be suppressed. However, the detailed mechanism of its quenching effect is poorly understood. In this study, we found that treating formaldehydefixed myocardial samples with 0.3 M glycine did not significantly change AF signal levels in both channels. There are two possible reasons: first, excessive free formaldehyde in myocardial samples was cleaned out during sucrose cryoprotection and wash procedures; second, formaldehyde cross-links were already formed before glycine could block them. Some preliminary results indicate that the quenching efficiency of glycine solutions can be improved by lowering the pH and/or increasing the concentration.¹⁹ However, lowering the pH is not practical for IF staining, as the pH of buffers has already been optimized for antibody sensitivity and affinity. Further experiments should be conducted to determine the efficacy of high-concentration glycine solutions on formaldehydefixed myocardial samples.

Unlike the treatments mentioned above, 0.1% and 1% NaBH₄ treatments were found to increase myocardial AF in both emission channels. One possible explanation for the increased AF could be the reduction of intracellular non-fluorescent NAD(P)+ to fluorescent NAD(P)H by NaBH₄. ^{32,33} With the development of label-free imaging methods and their demonstrated needs for cardiovascular research, AF contrast has been widely used by various microscopic

imaging techniques to detect intracellular and extracellular structures in the myocardium, such as widefield,³⁴ confocal,³⁵ multiphoton³⁶ and light-sheet³⁷. Our finding suggests the potential application of NaBH₄ as an AF enhancer in label-free imaging. This could facilitate the visualization of myocardial structures in image-based histological and histopathological studies without the need for laborious staining procedures. Further studies are required to verify whether NaBH₄-induced AF enhancement is specific to certain myocardial structures. When using NaBH₄, it is recommended to use freshly prepared solutions since NaBH₄ reacts with water and decomposes into non-functional sodium borate and hydrogen.

The varying reactivity of formaldehyde with proteins²⁰ and the inhomogeneous local distribution of endogenous fluorophores⁶ result in distinct AF contrasts across different structures in fixed tissues. We identified the major autofluorescent structures withing the formaldehyde-fixed myocardium, including mitochondria in cardiomyocytes, microvascular endothelial cells, and cardiac interstitium. Subsequently, we examined the quenching performance of SBB and TrueBlack® on these identified myocardial structures. We also inspected the AF enhancement performance of NaBH4 on these structures. SBB has been reported as an effective reagent for eliminating lipofuscin-like AF. 38,39 Lipofuscin commonly accumulates in lysosomes due to an aging effect in long-lived cells, 40 such as cardiomyocytes in our case. Nevertheless, we found SBB not only quenched autofluorescent lipofuscin granules in cardiomyocyte lysosomes but also completely eliminated AF from cardiomyocytes and microvessels. This finding is in line with the observation on paraffin sections of formaldehyde-fixed myocardium. 12 Moreover, SBB rendered autofluorescent structures invisible in both the pre-treatment and post-treatment protocols. Despite the excellent quenching performance, SBB significantly reduced IF labeling signal (far-red dye in this study). In contrast, TrueBlack® affected IF staining with a more acceptable reduction. When employing the pre-treatment protocol, TrueBlack[®] significantly reduced AF signal, yet major autofluorescent structures remained recognizable. When using the post-treatment protocol, TrueBlack® resulted in an evenly distributed AF background throughout the tissue area without any discernible features. Unlike SBB and TrueBlack[®], NaBH₄ resulted in a clearer visualization of mitochondria in cardiomyocytes and microvessel walls. The visibility of the endocardial layer was also notably improved, likely attributed to the enhanced AF contrast of endothelial cells lining the ventricular chambers. Further study should be conducted to identify the AF structures within the endocardial layer, which would provide a better understanding of the mechanism behind NaBH₄-induced AF enhancement.

In summary, SBB and TrueBlack® yielded the most efficient AF suppression on formaldehyde-fixed myocardial samples. SBB outperformed TrueBlack® in suppressing AF, and it entirely blacked out major autofluorescent structures in both the pre-treatment and post-treatment protocols. In contrast, TrueBlack® outperformed SBB in maintaining IF signal. Moreover, we found that NaBH₄ demonstrated a significant AF enhancement effect on major autofluorescent structures in myocardial samples, such as mitochondria in cardiomyocytes and microvessel walls, instead of suppressing AF as expected. This finding suggests that NaBH₄ has the potential to be used as an AF enhancer in label-free imaging. It may offer a counterstaining-free method to facilitate the interpretation of typical histological structures within the myocardium. The evaluation of these treatments was carried out on formaldehyde-fixed frozen sections, and their effectiveness on paraffin sections requires further validation.





Acknowledgments

We thank Dr. Robin C. Muise-Helmericks for sharing C57BL/6 mice and Fatemeh Nasehi for dissecting mice. We also thank Dr. Amy D. Bradshaw for providing CD31 primary antibodies.

References

- Bastiaens PIH, Pepperkok R. Observing proteins in their natural habitat: The living cell. Trends Biochem Sci 2000;25:631-7
- Yuan P, Condello C, Keene CD, Wang Y, Bird TD, Paul SM, et al. TREM2 haplodeficiency in mice and humans impairs the microglia barrier function leading to decreased amyloid compaction and severe axonal dystrophy. Neuron 2016;90:724-39.
- 3. Shi X, Garcia G, Van De Weghe JC, McGorty R, Pazour GJ, Doherty D, et al. Super-resolution microscopy reveals that disruption of ciliary transition-zone architecture causes Joubert syndrome. Nat Cell Biol 2017;19:1178-88.
- Wojnilowicz M, Glab A, Bertucci A, Caruso F, Cavalieri F. Super-resolution imaging of proton sponge-triggered rupture of endosomes and cytosolic release of small interfering RNA. ACS Nano 2019;13:187-202.
- Degors IMS, Wang C, Rehman ZU, Zuhorn IS. Carriers break barriers in drug delivery: endocytosis and endosomal escape of gene delivery vectors. Acc Chem Res 2019;52:1750-60.
- Wagnieres GA, Star WM, Wilson BC. In vivo fluorescence spectroscopy and imaging for oncological applications. Photochem Photobiol 1998;68:603-32.
- Corrodi HR, Jonsson G. The formaldehyde fluorescence method for the histochemical demonstration of biogenic monoamines a review on the methodology. J Histochem Cytochem 1967;15:65-78.
- 8. Ghasemi F, Parvin P, Lotfi M. Laser-induced fluorescence spectroscopy for diagnosis of cancerous tissue based on the fluorescence properties of formaldehyde. Laser Phys Lett 2019;16:35601.
- Clancy B, Cauller LJ. Reduction of background autofluorescence in brain sections following immersion in sodium borohydride. J Neurosci Methods 1998;83:97-102.
- Davis AS, Richter A, Becker S, Moyer JE, Sandouk A, Skinner J, et al. Characterizing and diminishing autofluorescence in formalin-fixed paraffin-embedded human respiratory tissue. J Histochem Cytochem 2014;62:405-23.
- 11. Lillie RD, Pizzolato P. Histochemical use of borohydrides as aldehyde blocking reagents. Stain Technol 1972;47:13-6.
- Baschong W, Suetterlin R, Laeng RH. Control of autofluorescence of archival formaldehyde-fixed, paraffin-embedded tissue in confocal laser scanning microscopy (CLSM). J Histochem Cytochem 2001;49:1565-71.
- Romijn HJ, van Uum JFM, Breedijk I, Emmering J, Radu I, Pool CW. Double immunolabeling of neuropeptides in the human hypothalamus as analyzed by confocal laser scanning fluorescence microscopy. J Histochem Cytochem 1999;47:229-35.
- 14. Oliveira VC, Carrara RC V, Simoes DLC, Saggioro FP, Carlotti CGJ, Covas DT, et al. Sudan Black B treatment reduces autofluorescence and improves resolution of in situ hybridization specific fluorescent signals of brain sections. Histol Histopathol 2010;25:1017-24.
- 15. Sun Y, Yu H, Zheng D, Cao Q, Wang Y, Harris D, et al. Sudan Black B reduces autofluorescence in murine renal tissue. Arch Pathol Lab Med 2011;135:1335-42.

- Kajimura J, Ito R, Manley NR, Hale LP. Optimization of single- and dual-color immunofluorescence protocols for formalin-fixed, paraffin-embedded archival tissues. J Histochem Cytochem 2015;64:112-24.
- 17. Erben T, Ossig R, Naim HY, Schnekenburger J. What to do with high autofluorescence background in pancreatic tissues an efficient Sudan black B quenching method for specific immunofluorescence labelling. Histopathology 2016;69:406-22.
- Wizenty J, Ashraf MI, Rohwer N, Stockmann M, Weiss S, Biebl M, et al. Autofluorescence: A potential pitfall in immunofluorescence-based inflammation grading. J Immunol Methods 2018;456:28-37.
- Sutherland BW, Toews J, Kast J. Utility of formaldehyde cross-linking and mass spectrometry in the study of proteinprotein interactions. J Mass Spectrom 2008;43:699-715.
- Hoffman EA, Frey BL, Smith LM, Auble DT. Formaldehyde crosslinking: a tool for the study of chromatin complexes. J Biol Chem 2015;290:26404-11.
- Yagi M, Toshima T, Amamoto R, Do Y, Hirai H, Setoyama D, et al. Mitochondrial translation deficiency impairs NAD+mediated lysosomal acidification. EMBO J 2021;40:e105268.
- Alex L, Tuleta I, Harikrishnan V, Frangogiannis NG. Validation of specific and reliable genetic tools to identify, label, and target cardiac pericytes in mice. J Am Heart Assoc 2022;11:e023171.
- Weckbach LT, Grabmaier U, Uhl A, Gess S, Boehm F, Zehrer A, et al. Midkine drives cardiac inflammation by promoting neutrophil trafficking and NETosis in myocarditis. J Exp Med 2019;216:350-68.
- 24. Zhang Z, Neff L, Bradshaw AD, Fan H, Ye E, Richardson W, et al. Multimodal microscopy imaging of cardiac collagen network: Are we looking at the same structures? Proc.SPIE 2023;12355:16.
- Piquereau J, Caffin F, Novotova M, Lemaire C, Veksler V, Garnier A, et al. Mitochondrial dynamics in the adult cardiomyocytes: Which roles for a highly specialized cell? Front Physiol 2013;4:102.
- 26. Kuznetsov A, Troppmair J, Sucher R, Hermann M, Saks V, Margreiter R. Mitochondrial subpopulations and heterogeneity revealed by confocal imaging: Possible physiological role? Biochim Biophys Acta 2006;1757:686-91.
- 27. Weber KT. Cardiac interstitium in health and disease: The fibrillar collagen network. J Am Coll Cardiol 1989;13:1637-52.
- 28. Karpishin T. Reducing tissue autofluorescence. Biotechniques 2018;64:131.
- Sakr N, Glazova O, Shevkova L, Onyanov N, Kaziakhmedova S, Shilova A, et al. Characterizing and quenching autofluorescence in fixed mouse adrenal cortex tissue. Int J Mol Sci 2023;24:3432.
- Kuo M-H, Allis CD. In vivo cross-linking and immunoprecipitation for studying dynamic protein: DNA associations in a chromatin environment. Methods 1999;19:425-33.
- 31. Vasilescu J, Guo X, Kast J. Identification of protein-protein interactions using in vivo cross-linking and mass spectrometry. Proteomics 2004;4:3845-54.
- Werner DA, Huang CC, Aminoff D. Micro method for determination of borohydride with NAD+. Anal Biochem 1973;54:554-60.
- Avigad G. Reduction of nicotinamide adenine dinucleotides by sodium cyanoborohydride. Biochim Biophys Acta - Enzymol 1979;571:171-4.
- Jensen T, Holten-Rossing H, Svendsen IMH, Jacobsen C, Vainer B. Quantitative analysis of myocardial tissue with digital autofluorescence microscopy. J Pathol Inform 2016;7:15.





- 35. Miller CE, Thompson RP, Bigelow MR, Gittinger G, Trusk TC, Sedmera D. Confocal imaging of the embryonic heart: How deep? Microsc Microanal 2005;11:216-23.
- King KR, Aguirre AD, Ye Y-X, Sun Y, Roh JD, Ng RP, et al. IRF3 and type I interferons fuel a fatal response to myocardial infarction. Nat Med 2017;23:1481-7.
- Ding Y, Lee J, Ma J, Sung K, Yokota T, Singh N, et al. Lightsheet fluorescence imaging to localize cardiac lineage and protein distribution. Sci Rep 2017;7:42209.
- 38. Schnell SA, Staines WA, Wessendorf MW. Reduction of lipo-

- fuscin-like autofluorescence in fluorescently labeled tissue. J Histochem Cytochem 1999;47:719-30.
- Viegas MS, Martins TC, Seco F, do Carmo A. An improved and cost-effective methodology for the reduction of autofluorescence in direct immunofluorescence studies on formalinfixed paraffin-embedded tissues. Eur J Histochem 2007;51:59-66
- 40. Terman A, Brunk UT. Lipofuscin: mechanisms of formation and increase with age. APMIS 1998;106:265-76.

Online supplementary material:

Widefield fluorescence microscopy

Figure S1. Widefield IF and AF images of control and samples treated with 0.3% SBB, TrueBlack®, and 1% NaBH₄ using the pre-treatment application protocol.

Figure S2. Widefield IF and AF images of control and samples treated with 0.3% SBB, TrueBlack*, and 1% NaBH₄ using the post-treatment application protocol.

Received for publication: 21 June 2023. Accepted for publication: 28 August 2023.

This work is licensed under a Creative Commons Attribution-NonCommercial 4.0 International License (CC BY-NC 4.0).

©Copyright: the Author(s), 2023 Licensee PAGEPress, Italy

European Journal of Histochemistry 2023; 67:3812

doi:10.4081/ejh.2023.3812

Publisher's note: all claims expressed in this article are solely those of the authors and do not necessarily represent those of their affiliated organizations, or those of the publisher, the editors and the reviewers. Any product that may be evaluated in this article or claim that may be made by its manufacturer is not guaranteed or endorsed by the publisher.

